

# The Genetic and Physical Interactomes of the *Saccharomyces cerevisiae* Hrq1 Helicase

Cody M. Rogers,\* Elsbeth Sanders,\* Phoebe A. Nguyen,\* Whitney Smith-Kinnaman,† Amber L. Mosley,† and Matthew L. Bochman\*<sup>2</sup>

\*Molecular and Cellular Biochemistry Department, Indiana University, Bloomington, IN 47405 and †Department of Biochemistry and Molecular Biology, Indiana University School of Medicine, Indianapolis, IN 46202

ORCID IDs: 0000-0001-5822-2894 (A.L.M.); 0000-0002-2807-0452 (M.L.B.)

**ABSTRACT** The human genome encodes five RecQ helicases (RECQL1, BLM, WRN, RECQL4, and RECQL5) that participate in various processes underpinning genomic stability. Of these enzymes, the disease-associated RECQL4 is comparatively understudied due to a variety of technical challenges. However, *Saccharomyces cerevisiae* encodes a functional homolog of RECQL4 called Hrq1, which is more amenable to experimentation and has recently been shown to be involved in DNA inter-strand crosslink (ICL) repair and telomere maintenance. To expand our understanding of Hrq1 and the RecQ4 subfamily of helicases in general, we took a multi-omics approach to define the Hrq1 interactome in yeast. Using synthetic genetic array analysis, we found that mutations of genes involved in processes such as DNA repair, chromosome segregation, and transcription synthetically interact with deletion of *HRQ1* and the catalytically inactive *hrq1-K318A* allele. Pull-down of tagged Hrq1 and mass spectrometry identification of interacting partners similarly underscored links to these processes and others. Focusing on transcription, we found that *hrq1* mutant cells are sensitive to caffeine and that mutation of *HRQ1* alters the expression levels of hundreds of genes. In the case of *hrq1-K318A*, several of the most highly upregulated genes encode proteins of unknown function whose expression levels are also increased by DNA ICL damage. Together, our results suggest a heretofore unrecognized role for Hrq1 in transcription, as well as novel members of the Hrq1 ICL repair pathway. These data expand our understanding of RecQ4 subfamily helicase biology and help to explain why mutations in human RECQL4 cause diseases of genomic instability.

## KEYWORDS

DNA helicase  
RecQ  
Hrq1  
*Saccharomyces cerevisiae*  
transcription

A multitude of cellular processes are necessary to ensure the maintenance of genome integrity, including high fidelity DNA replication, recombination and repair, telomere maintenance, and transcription. Among the proteins that are involved, DNA helicases represent one of only a few enzyme classes that are vital to all of these processes

(Bochman 2014). Helicases are enzymes that use the power of ATP hydrolysis to drive conformational changes that enable translocation along DNA and unwinding of DNA base pairs (Abdelhaleem 2010; Brosh and Matson 2020). Because these enzymes are involved in so many critical functions *in vivo*, it is unsurprising that mutations in genes encoding helicases are causative of or linked to numerous diseases of genomic instability such as cancer and aging (Monnat 2010; Suhasini and Brosh 2013; Uchiumi *et al.* 2015).

Despite their prominent roles in maintaining genome integrity however, we often lack a detailed understanding of why a particular mutation in a helicase is associated with a pathological disorder. In other words, what cellular processes are impacted that eventually precipitate a disease state when a helicase is mutated? Part of the difficulty in answering this question is that many helicases are multi-functional, and a defect in any one of a number of functions could cause genomic instability (Hickson 2003). Another issue is that helicases are numerous, with > 100 predicted to be encoded by typical eukaryotic genomes (Eki 2010), and many helicases share

Copyright © 2020 Rogers *et al.*

doi: <https://doi.org/10.1534/g3.120.401864>

Manuscript received August 27, 2020; accepted for publication October 23, 2020; published Early Online October 28, 2020.

This is an open-access article distributed under the terms of the Creative Commons Attribution 4.0 International License (<http://creativecommons.org/licenses/by/4.0/>), which permits unrestricted use, distribution, and reproduction in any medium, provided the original work is properly cited.

Supplemental material available at figshare: <https://doi.org/10.25387/g3.13154291>.

<sup>1</sup>Present address: Cody M. Rogers, Department of Biochemistry and Structural Biology, University of Texas Health Science Center at San Antonio, San Antonio, TX 78229

<sup>2</sup>Corresponding author: 212 S. Hawthorne Dr., Simon Hall MSB1 room 405B, Bloomington, IN 47405. E-mail: [bochman@indiana.edu](mailto:bochman@indiana.edu)

partially redundant or backup roles, which complicates identification of phenotypes without thorough genomic or proteomic approaches.

One such under-studied and disease-linked helicase is the human RECQL4 protein. Dozens of mutant alleles of *RECQL4* cause three different diseases (Baller-Gerold syndrome (Van Maldergem *et al.* 1993), RAPADILINO (Vargas *et al.* 1992), and Rothmund-Thomson syndrome (Liu 2010)) characterized by a predisposition to cancers, but it is unclear why these mutations cause disease. RECQL4 is difficult to study *in vivo* because it is an evolutionary chimera between a RecQ family helicase and Sld2 (Capp *et al.* 2010), an essential DNA replication initiation factor in lower eukaryotes (Kamimura *et al.* 1998). Helicase activity by RECQL4 is not needed for DNA replication, but pleiotropic defects in replication hamper the analysis of the roles of the helicase domain when studying *recq4* mutants. Similarly, RECQL4 is difficult to study *in vitro* because the protein is large (~135 kD) with a natively disordered N-terminus (Keller *et al.* 2014), making the generation of recombinant protein for biochemistry arduous (Macris *et al.* 2006; Bochman *et al.* 2014). Thus, although RECQL4 is reported to be involved in telomere maintenance (Ghosh *et al.* 2011) and DNA inter-strand crosslink (ICL) repair (Jin *et al.* 2008; Rogers *et al.* 2020b), its mechanism of action in these pathways is unknown.

Recently, we established the *Saccharomyces cerevisiae* Hrq1 helicase as a functional homolog of the helicase portion of RECQL4, showing that it too is linked to telomere maintenance and ICL repair (Bochman *et al.* 2014; Rogers and Bochman 2017; Rogers *et al.* 2017; Nickens *et al.* 2018; Nickens *et al.* 2019; Rogers *et al.* 2020a). However, because Sld2 is a separate protein in *S. cerevisiae* and recombinant Hrq1 is more amenable to biochemistry, we have been able to delve into the molecular details of Hrq1 in the maintenance of genome integrity. For instance, Hrq1 synergizes with the helicase Pif1 to regulate telomerase activity, likely establishing telomere length homeostasis *in vivo* (Nickens *et al.* 2018). In ICL repair, Hrq1 stimulates the translesional nuclease activity of Pso2 to aid in remove of the ICL (Rogers *et al.* 2020a). During the course of these investigations, we have also found that alleles of *HRQ1* genetically interact with mutations in the gene encoding the other RecQ family helicase in *S. cerevisiae*, *SGS1* (Bochman *et al.* 2014), and that Hrq1 may be involved in the maintenance of DNA motifs capable of forming G-quadruplex (G4) structures (Rogers *et al.* 2017). These facts are mirrored by the interaction of RECQL4 with the human Sgs1 homolog BLM (Singh *et al.* 2012) and the ability of RECQL4 to bind to and unwind G4 DNA (Keller *et al.* 2014).

To gain a more comprehensive understanding of the roles of RecQ4 subfamily helicases in genome integrity, we sought to define the Hrq1 interactome in yeast. In a companion manuscript (Sanders, Nguyen *et al.*; manuscript #401709), we performed synthetic genetic array (SGA) analysis of *hrq1Δ* and *hrq1-K318A* (catalytically inactive mutant) cells using the yeast deletion collection and the temperature-sensitive (TS) collection. Here, hundreds of significant positive and negative interactions were identified, with gene ontology (GO) term enrichment for processes such as transcription and rRNA processing in addition to expected functions such as DNA repair. Mass spectrometry (MS) analysis of proteins that physically interact with Hrq1 returned similar results. Our initial characterization of the link between Hrq1 and transcription revealed that *hrq1* mutant cells are sensitive to the transcription stressor caffeine and that the *hrq1Δ* and *hrq1-K318A* mutations affect the transcription of hundreds of

genes, many of which are known or hypothesized to be related to transcription, DNA ICL repair, and the cytoskeleton.

## MATERIALS AND METHODS

### Strain construction

The *HRQ1* gene was deleted in Y8205 (Table 1) by transforming in a NatMX cassette that was PCR-amplified from plasmid pAC372 (a gift from Amy Caudy) using oligonucleotides MB525 and MB526 (Table S1). The deletion was verified by PCR analysis using genomic DNA and oligonucleotides that anneal to regions up- and downstream of the *HRQ1* locus (MB527 and MB528). The confirmed *hrq1Δ* strain was named MBY639. The *hrq1-K318A* allele was introduced into the Y8205 background in a similar manner. First, an *hrq1-K318A(NatMX)* cassette was PCR-amplified from the genomic DNA of strain MBY346 (Bochman *et al.* 2014) using oligonucleotides MB527 and MB528 and transformed into Y8205. Then, genomic DNA was prepared from transformants and used for PCR analyses of the *HRQ1* locus with the same oligonucleotide set to confirm insertion of the NatMX marker. Finally, PCR products of the expected size for *hrq1-K318A(NatMX)* were sequenced using oligonucleotide MB932 to confirm the presence of the K318A mutation. The verified *hrq1-K318A* strain was named MBY644. Hrq1 was tagged with a 3xFLAG epitope in the YPH499 genetic background by transformation of a 3xFLAG(His3MX6) cassette that was PCR-amplified from the pFA6a-3xFLAG-His3MX6 plasmid (Funakoshi and Hochstrasser 2009) using oligonucleotides MB1028 and MB1029. Proper integration was assessed by PCR and sequencing as described above for *hrq1-K318A(NatMX)*. The confirmed Hrq1-3xFLAG strain was named MBY520.

### SGA analysis

SGA analysis of the *hrq1Δ* and *hrq1-K318A* alleles was performed at the University of Toronto using previously described methods (Tong *et al.* 2001; Tong *et al.* 2004). The *hrq1* mutants were crossed to both the *S. cerevisiae* single-gene deletion collection (Giaever and Nislow 2014) and the TS alleles collection (Kofoed *et al.* 2015) to generate double mutants for analysis. Quantitative scoring of the genetic interactions was based on colony size. The SGA score measures the extent to which a double mutant colony size deviates from the colony size expected from combining two mutations together. The data include both negative (putative synthetic sick/lethal) and positive interactions (potential epistatic or suppression interactions) involving *hrq1Δ* and *hrq1-K318A*. The magnitude of the SGA score is indicative of the strength of the interaction. Based on statistical analysis, it was determined that a default cutoff for a significant genetic interaction is  $P < 0.05$  and SGA score  $> |0.08|$ . It should be noted that only top-scoring interactions were confirmed by remaking and reanalyzing the double mutants by hand. The full SGA data are available in our companion manuscript (Sanders, Nguyen, *et al.*; manuscript #401709).

### Confirmation of top SGA hits

The top five positive and negative interactors with *hrq1Δ* and *hrq1-K318A* from the single-gene deletion and TS arrays were reanalyzed by hand to confirm their phenotypes. Briefly, the SGA query strains MBY639 and MBY644 (Nat<sup>R</sup>) were mated to *MATa* tester strains from the arrays (Kan<sup>R</sup>), sporulated, and then analyzed by random spore analysis (Lichten 2014), spot dilution (Andis *et al.* 2018), and/or growth curve (Ononye *et al.* 2020) assays and/or growth curve analyses of Nat<sup>R</sup> Kan<sup>R</sup> spore clones compared to the parental single-mutant strains and wild-type.

■ **Table 1** Strains used in this study

Name	Genotype	Source
Y8205	<i>MAT<math>\alpha</math> can1<math>\Delta</math>::STE2pr-Sp_his5 lyp1<math>\Delta</math>::STE3pr-LEU2 his3<math>\Delta</math>1 leu2<math>\Delta</math>0 ura3<math>\Delta</math>0</i>	(Tong <i>et al.</i> 2001)
YPH499	<i>MAT<math>\alpha</math> ura3-52 lys2-801_amber ade2-101_ochre trp1<math>\Delta</math>63 his3<math>\Delta</math>200 leu2<math>\Delta</math>1</i>	(Sikorski and Hieter 1989)
MBY346	<i>MAT<math>\alpha</math> ura3-52 lys2-801_amber ade2-101_ochre trp1<math>\Delta</math>63 his3<math>\Delta</math>200 leu2<math>\Delta</math>1 hxt13::URA3 hrq1::hrq1-K318A-NatMX</i>	(Bochman <i>et al.</i> 2014)
MBY520	<i>MAT<math>\alpha</math> ura3-52 lys2-801_amber ade2-101_ochre trp1<math>\Delta</math>63 his3<math>\Delta</math>200 leu2<math>\Delta</math>1 HRQ1:3xFLAG-His3MX6</i>	This study
MBY639	<i>MAT<math>\alpha</math> can1<math>\Delta</math>::STE2pr-Sp_his5 lyp1<math>\Delta</math>::STE3pr-LEU2 his3<math>\Delta</math>1 leu2<math>\Delta</math>0 ura3<math>\Delta</math>0 hrq1::NatMX</i>	This study
MBY644	<i>MAT<math>\alpha</math> can1<math>\Delta</math>::STE2pr-Sp_his5 lyp1<math>\Delta</math>::STE3pr-LEU2 his3<math>\Delta</math>1 leu2<math>\Delta</math>0 ura3<math>\Delta</math>0 hrq1::hrq1-K318A(NatMX)</i>	This study

### Hrq1-3xFLAG affinity pulldown

To immunoprecipitate Hrq1-3xFLAG and its associated proteins, strain MBY520 was grown to an optical density at 600 nm ( $OD_{600}$ ) of  $\sim 1.5$  in YPD medium at 30° with shaking. The cells were harvested by centrifugation at 4°, washed with 50 mL of sterile ice-cold H<sub>2</sub>O, and harvested as before. The cell pellet was then resuspended in 100  $\mu$ L/g of cells resuspension buffer (20 mM Na-HEPES, pH 7.5, and 1.2% w/v PEG-8000) supplemented with 10  $\mu$ g/mL DNase I and protease inhibitor cocktail (600 nM leupeptin, 2  $\mu$ M pepstatin A, 2 mM benzamidine, and 1 mM phenylmethanesulfonyl fluoride). This cell slurry was slowly dripped into liquid nitrogen to generate frozen yeast “popcorn”, which was stored at -80° until use. To cryo-lyse the cells, the popcorn was ground in a freezer mill with dry ice. The resultant powder was collected into 50-mL conical tubes that were loosely capped and stored at -80° overnight to allow the dry ice to sublimate away. To perform the Hrq1 pull down, the cell powder was resuspended in 2.5 g powder per 25 mL lysis buffer (40 mM Na-HEPES, pH 7.5, 10% glycerol, 350 mM NaCl, 0.1% Tween-20, and protease inhibitor cocktail) with gentle agitation. Then, 100 U DNase I and 10  $\mu$ L of 30 mg/mL heparin were added, and the sample was incubated for 10 min at room temperature with gentle agitation. Cellular debris was pelleted by centrifugation at 14,000  $\times$  g for 10 min at 4°. Then, 100  $\mu$ L of anti-FLAG agarose slurry was washed and equilibrated with lysis buffer, and the clarified lysate and anti-FLAG resin were added to a fresh 50-mL conical tube. This suspension was incubated at 4° overnight on a nutator. The resin and lysate were subsequently placed in a 30-mL chromatography column, and the lysate was allowed to flow through the resin by gravity. The anti-FLAG agarose was washed with 30 mL lysis buffer, and the beads were then resuspended in 150  $\mu$ L lysis buffer and transferred to a 1.5-mL microcentrifuge tube. At this point, the sample could be used for proteinase digestion and MS analysis, or proteins could be eluted from the resin and examined by SDS-PAGE and Coomassie staining. The untagged control strain (MBY4) was also processed as above to identify proteins that nonspecifically bound to the anti-FLAG agarose.

### Label-free quantitative proteomics interactome analysis

For on-bead digestion, 500  $\mu$ L of trypsin digestion buffer (50 mM NH<sub>4</sub>HCO<sub>3</sub>, pH 8.5) was used to resuspend the FLAG resin. To this slurry, 10  $\mu$ L of 0.1  $\mu$ g/ $\mu$ L Trypsin Gold (Promega) was added and allowed to incubate overnight at 37° with shaking. After digestion, the FLAG resin was separated from the digested peptides via spin columns and centrifugation. Formic acid (0.1% final concentration) was added to the supernatant to quench the reaction. After digestion, the peptide mix was separated into three equal aliquots. Each replicate

was then loaded onto a microcapillary column. Prior to sample loading, the microcapillary column was packed with three phases of chromatography resin: reverse phase resin, strong cation resin, and reverse phase resin, as previously described (Florens and Washburn 2006; Mosley *et al.* 2011; Mosley *et al.* 2013). An LTQ Velos Pro with an in-line Proxeon Easy nLC was utilized for each technical replicate sample, with a 10-step MudPIT method. In MS1, the 10 most intense ions were selected for MS/MS fragmentation, using collision induced dissociation (CID). Dynamic exclusion was set to 90 s with a repeat count of one. Protein database matching of RAW files was performed using SEQUEST and Proteome Discoverer 2.2 (Thermo) against a FASTA database from the yeast Uniprot proteome. Database search parameters were as follows: precursor mass tolerance = 1.4 Da, fragment mass tolerance = 0.8 Da, up to two missed cleavages were allowed, enzyme specificity was set to fully tryptic, and minimum peptide length = 6 amino acids. The false discovery rate (FDR) for all spectra was <1% for reporting as PSM. Percolator, within Proteome Discoverer 2.2, was used to calculate the FDR (Käll *et al.* 2007). SAINT probability scores were calculated as outlined in the Contaminant Repository for Affinity Purification (CRAPome) website (Mellacheruvu *et al.* 2013) and other publications ((Breitkreutz *et al.* 2010; Choi *et al.* 2011; Choi *et al.* 2012; Kwon *et al.* 2013).

### Caffeine sensitivity

The sensitivity of *hrq1* mutant cells to caffeine was assessed both qualitatively and quantitatively. In the first method, cells of the indicated strains were grown overnight in YPD medium at 30° with aeration, diluted to  $OD_{600} = 1$  in sterile H<sub>2</sub>O, and then serially diluted 10-fold to 10<sup>-4</sup>. Five microliters of these dilutions were then spotted onto YPD agar plates and YPD agar plates supplemented with 10 mM caffeine. The plates were incubated at 30° for 2 days before capturing images with a flatbed scanner and scoring growth. In the second method, the overnight cultures were diluted to  $OD_{600} = 0.01$  into YPD or YPD supplemented with various concentrations of caffeine. They were then treated as described in (Ononye *et al.* 2020) with slight modifications. Briefly, 200  $\mu$ L of each culture was placed in duplicate into wells in 96-well plates, and each well was overlaid with mineral oil to prevent evaporation. The plates were incubated (30° with shaking) in a Synergy <sup>1</sup>H microplate reader (BioTek), which recorded  $OD_{660}$  measurements at 15-min intervals for 24 h. The mean of the  $OD_{660}$  readings for each strain was divided by the mean  $OD_{660}$  of the same strain grown in YPD.

### RNA-seq

Cells were harvested from mid-log phase cultures grown in YPD medium, and total RNA was prepared using a YeaStar RNA kit (Zymo

Research). Sequencing libraries were prepared, and Illumina sequencing was performed by, Novogene Corporation. Data analysis was then performed by the Indiana University Center for Genomics and Bioinformatics. The sequences were trimmed using the Trim Galore script ([https://www.bioinformatics.babraham.ac.uk/projects/trim\\_galore/](https://www.bioinformatics.babraham.ac.uk/projects/trim_galore/)), and reads were mapped to the *S. cerevisiae* genome using bowtie2 on local mode (Langmead and Salzberg 2012). Reads were counted, and differential expression analysis were performed using DESeq2 (Love *et al.* 2014). Two or three independent replicates of each strain were analyzed.

### Statistical analysis

Data were analyzed and graphed using GraphPad Prism 6 software. The reported values are averages of <sup>3</sup> 3 independent experiments, and the error bars are the standard deviation. *P*-values were calculated as described in the figure legends, and we defined statistical significance as *P* < 0.01.

### Data availability

Strains, plasmids, RNA-seq data, and other experimental reagents are available upon request. File S1 contains detailed descriptions of all

supplemental files, as well as Table S1 and Figure S1. File S2 contains the significant SGA hits. File S3 contains the full SAINT analysis results. File S4 contains the transcriptomic changes identified by RNA-seq. Supplemental material available at figshare: <https://doi.org/10.25387/g3.13154291>.

## RESULTS AND DISCUSSION

### The genetic interactome of HRQ1

In a companion study (Sanders, Nguyen, *et al.*; manuscript #401709), we crossed the *hrq1Δ* and *hrq1-K318A* alleles to the single-gene deletion and TS allele collections to generate all possible double mutants and assessed the growth of the resulting spore clones to identify negative and positive genetic interactions. A discussion of the significant positive and negative genetic interactions can be found therein. Here, we used GO Term mapping to identify cellular processes enriched for *hrq1* genetic interactors in those data. These processes were similar when considering the *hrq1Δ* and *hrq1-K318A* datasets alone or together, so we present the combined results for simplicity. For all of the negative genetic interactions with *hrq1Δ* and *hrq1-K318A*, the top 10 GO terms were transcription by RNA polymerase

■ **Table 2 Gene Ontology (GO) Term enrichment of negative genetic interactors with *hrq1***

GO Term (GO ID)	Genes Annotated to the GO Term	GO Term Usage in Gene List	Genome Frequency of Use
transcription by RNA polymerase II (GO:0006366)	ABF1, CDC28, CDC73, CEG1, CSE2, EAF7, ESS1, GIM3, HMO1, HTZ1, MED11, NAB3, NUT1, RAD4, SDS3, SGF73, SIN3, SPT15, SPT3, SPT8, SRB2, SRB6, STH1, SUA7, SWI4, TAF11, TAF2, YJR084W	28 of 191 genes, 14.66%	536 of 6436 annotated genes, 8.33%
regulation of organelle organization (GO:0033043)	APC4, BDF2, CDC15, CDC20, CDC28, CDC73, CTI6, DAM1, EFB1, ESS1, GIC1, LTE1, MOB1, PEF1, PSE1, SDS3, SIN3, SPO16, TGS1, UTH1, VPS41	21 of 191 genes, 10.99%	326 of 6436 annotated genes, 5.07%
DNA repair (GO:0006281)	ABF1, ACT1, BDF2, CDC28, CDC73, CST9, EAF7, NSE4, NSE5, POL1, PRP19, RAD14, RAD33, RAD4, RAD52, RAD54, RAD59, RNH201, RTT107, SIN3, STH1	21 of 191 genes, 10.99%	300 of 6436 annotated genes, 4.66%
chromatin organization (GO:0006325)	ABF1, BDF2, CDC28, CLP1, CTI6, EAF7, ESS1, GIC1, HTZ1, LGE1, RAD54, SDS3, SGF73, SIN3, SIR1, SPT3, SPT8, STH1, SWC5, UTH1, YCS4	21 of 191 genes, 10.99%	310 of 6436 annotated genes, 4.82%
mitotic cell cycle (GO:0000278)	ACT1, APC4, CDC10, CDC15, CDC20, CDC25, CDC28, CDC34, DAM1, GIC1, LTE1, MOB1, PEF1, POL1, PSE1, SIC1, SIN3, SWI4, TUB2, YCS4	20 of 191 genes, 10.47%	373 of 6436 annotated genes, 5.80%
peptidyl-amino acid modification (GO:0018193)	ACT1, APJ1, CDC15, CDC28, CDC73, CST9, DBF2, EAF7, ESS1, LIP5, NSE4, NSE5, PSE1, SGF73, SMT3, SPO16, SPT3, SPT8, SWF1, TDA1	20 of 191 genes, 10.47%	244 of 6436 annotated genes, 3.79%
cytoskeleton organization (GO:0007010)	ACT1, BBP1, CDC10, CDC15, CDC28, CDC31, CMD1, CTF13, DAM1, EFB1, ENT1, ENT3, GIC1, NDC1, SPC29, STH1, SWF1, TUB2	18 of 191 genes, 9.42%	272 of 6436 annotated genes, 4.23%
mitochondrion organization (GO:0007005)	ACT1, ATG1, ATG3, COA4, FCJ1, MDM35, PAM16, PAM17, PHB2, PTC1, QCR2, RCF2, SAM37, TIM18, TOM70, UTH1, YJR120W, YME1	18 of 191 genes, 9.42%	279 of 6436 annotated genes, 4.33%
organelle fission (GO:0048285)	APC4, CDC10, CDC15, CDC20, CDC28, CST9, DAM1, DBF2, EBP2, GIC1, LTE1, MOB1, PSE1, RAD52, SPO16, TUB2, YCS4	17 of 191 genes, 8.90%	268 of 6436 annotated genes, 4.16%
response to chemical (GO:0042221)	ACT1, ASK10, GIM3, GPR1, IRA2, MUP3, PTC1, SRB2, TDA1, TIM18, TMA19, TUB2, VPS27, YJR084W, YLR225C, YOS9	16 of 191 genes, 8.38%	567 of 6436 annotated genes, 8.81%

II, regulation of organelle organization, DNA repair, chromatin organization, mitotic cell cycle, peptidyl-amino acid modification, cytoskeleton organization, mitochondrion organization, organelle fission, and response to chemical (Table 2). Similarly, for all of the positive genetic interactions with *hrq1Δ* and *hrq1-K318A*, the top 10 GO terms were mitotic cell cycle, cytoskeleton organization, regulation of organelle organization, lipid metabolic process, DNA repair, transcription by RNA polymerase II, chromatin organization, chromosome segregation, organelle fission, and rRNA processing (Table 3). The DNA repair-related genes were not enriched for known or putative ICL repair genes as one might expect considering the ICL sensitivity phenotypes of *hrq1Δ* and *hrq1-K318A* cells. However, a chemogenomics screen exposing all of the double mutants from these SGA screens to one or more ICL-inducing compounds may provide such hits and new insights into ICL repair in *S. cerevisiae*, and such follow-up screens are planned for the future.

A discussion of the strongest negative synthetic genetic interactions with *hrq1Δ* and *hrq1-K318A* is included in our companion manuscript (Sanders, Nguyen, *et al.*; manuscript #401709). Briefly, this included synthetic interactions with genes encoding genome integrity factors (*e.g.*, *RAD14* and *CBC2*) and mitochondrial proteins (*e.g.*, *MRM2* and *TOM70*), consistent with the known roles of Hrq1 and human RECQL4 in genome maintenance (Ghosh *et al.* 2011; Singh *et al.* 2012; Choi *et al.* 2013; Bochman *et al.* 2014; Choi *et al.* 2014; Leung *et al.* 2014; Rogers *et al.* 2017; Nickens *et al.* 2018; Rogers *et al.* 2020a) and their nuclear and mitochondrial localization (Croteau *et al.* 2012; Koh *et al.* 2015; Kumari *et al.* 2016).

Deletion alleles of *ARP8* and *SHE1* and TS alleles of *ACT1*, *ARP3*, *CSE2*, *MPS1*, and *MPS3* are among the strongest positive synthetic genetic interactors with *hrq1Δ* and/or *hrq1-K318A* (Tables S3 and S5). *Arp8* is a chromatin remodeling factor (Shen *et al.* 2000), and *Cse2* is a Mediator complex subunit required for RNA polymerase II regulation (Gustafsson *et al.* 1998), consistent with the GO Term enrichment described above. This may suggest that like human RECQL5 (Aygün *et al.* 2008; Izumikawa *et al.* 2008; Saponaro *et al.* 2014), Hrq1 plays a role in transcription.

*She1* is a microtubule-associated protein (Bergman *et al.* 2012), as is human RECQL4 (Yokoyama *et al.* 2019). Likewise, *Mps1* and *Mps3* are linked to the microtubule cytoskeleton as proteins necessary for spindle pole body function (Friederichs *et al.* 2011; Meyer *et al.* 2013). We attempted to determine if Hrq1 also binds to microtubules using an *in vitro* microtubule co-sedimentation assay (Walker *et al.* 2019), but found that Hrq1 alone pellets during ultracentrifugation (data not shown). We hypothesize that this is due to the natively disordered N-terminus of Hrq1 (Rogers *et al.* 2017; Rogers *et al.* 2020a), which may mediate liquid-liquid phase separation (LLPS) of recombinant Hrq1 in solution. Ongoing experiments are addressing the LLPS of Hrq1 alone and in combination with its ICL repair cofactor Pso2 (Rogers *et al.* 2020a).

*ACT1* encodes the *S. cerevisiae* actin protein (Gallwitz and Seidel 1980), and *Arp3* is a subunit of the Arp2/3 complex that acts as an actin nucleation center (Machesky and Gould 1999). It is unclear why mutation of these cytoskeletal factors yields increased growth in combination with *hrq1* mutations. However, *arp3* mutation also decreases telomere length (Ungar *et al.* 2009). Thus, this synthetic

■ Table 3 Gene Ontology (GO) Term enrichment of positive genetic interactors with *hrq1*

GO Term (GO ID)	Genes Annotated to the GO Term	GO Term Usage in Gene List	Genome Frequency of Use
mitotic cell cycle (GO:0000278)	ACT1, APC11, BRN1, CDC48, CDC6, CLB3, CSM1, DPB11, IPL1, MCD1, MPS1, MPS3, MYO2, PDS5, PFY1, PSE1, PSF1, SMC4, SPT6, VRP1	20 of 151 genes, 13.25%	373 of 6436 annotated genes, 5.80%
cytoskeleton organization (GO:0007010)	ACT1, AIM14, ARP3, CDC48, CLB3, ICE2, IPL1, LAS17, MPS1, MPS2, MPS3, MYO2, NUM1, PFY1, RSP5, SPC29, STH1, TSC11, VRP1	19 of 151 genes, 12.58%	272 of 6436 annotated genes, 4.23%
regulation of organelle organization (GO:0033043)	AIM14, APC11, ARP3, CDC48, CDC6, CLB3, IPL1, LAS17, MPS1, PCP1, PFY1, PSE1, RSP5, SEC23, SGV1, SPT6, TSC11, VRP1	18 of 151 genes, 11.92%	326 of 6436 annotated genes, 5.07%
lipid metabolic process (GO:0006629)	ALG14, CDC1, CHO2, DGA1, GAA1, GPI10, GPI12, GPI2, GWT1, LCB1, MGA2, OPI3, PHS1, RSP5, SAC1, SUR1, TSC11, VPS4	18 of 151 genes, 11.92%	347 of 6436 annotated genes, 5.39%
DNA repair (GO:0006281)	ACT1, ARP8, CDC1, DPB11, IXR1, MCD1, NHP10, PDS5, POB3, POL3, PSF1, RAD3, RNH201, RSC2, SLX5, SLX8, STH1, TEL1	18 of 151 genes, 11.92%	300 of 6436 annotated genes, 4.66%
transcription by RNA polymerase II (GO:0006366)	CAM1, CSE2, IXR1, MGA2, MOT1, NHP10, PDC2, POB3, RAD3, RGR1, RSC2, RSP5, SGV1, SPT6, STH1	15 of 151 genes, 9.93%	536 of 6436 annotated genes, 8.33%
chromatin organization (GO:0006325)	ARP8, CAC2, CDC6, IES1, MGA2, MPS3, NHP10, ORC6, POB3, RSC2, RSP5, SPT6, STH1, TEL1	14 of 151 genes, 9.27%	310 of 6436 annotated genes, 4.82%
chromosome segregation (GO:0007059)	APC11, BRN1, CDC48, CSM1, IPL1, MCD1, MPS1, MPS3, PDS5, RSC2, SMC4, SPC24, STH1	13 of 151 genes, 8.61%	210 of 6436 annotated genes, 3.26%
organelle fission (GO:0048285)	APC11, BRN1, CLB3, CSM1, IPL1, MCD1, MPS1, MPS3, NUM1, PDS5, PSE1, SMC4	12 of 151 genes, 7.95%	268 of 6436 annotated genes, 4.16%
rRNA processing (GO:0006364)	BMS1, FAL1, MAK5, MOT1, MRM2, POP4, RPF2, RPS23A, RPS6B, RPS9B, RSP5, SLX9	12 of 151 genes, 7.95%	352 of 6436 annotated genes, 5.47%

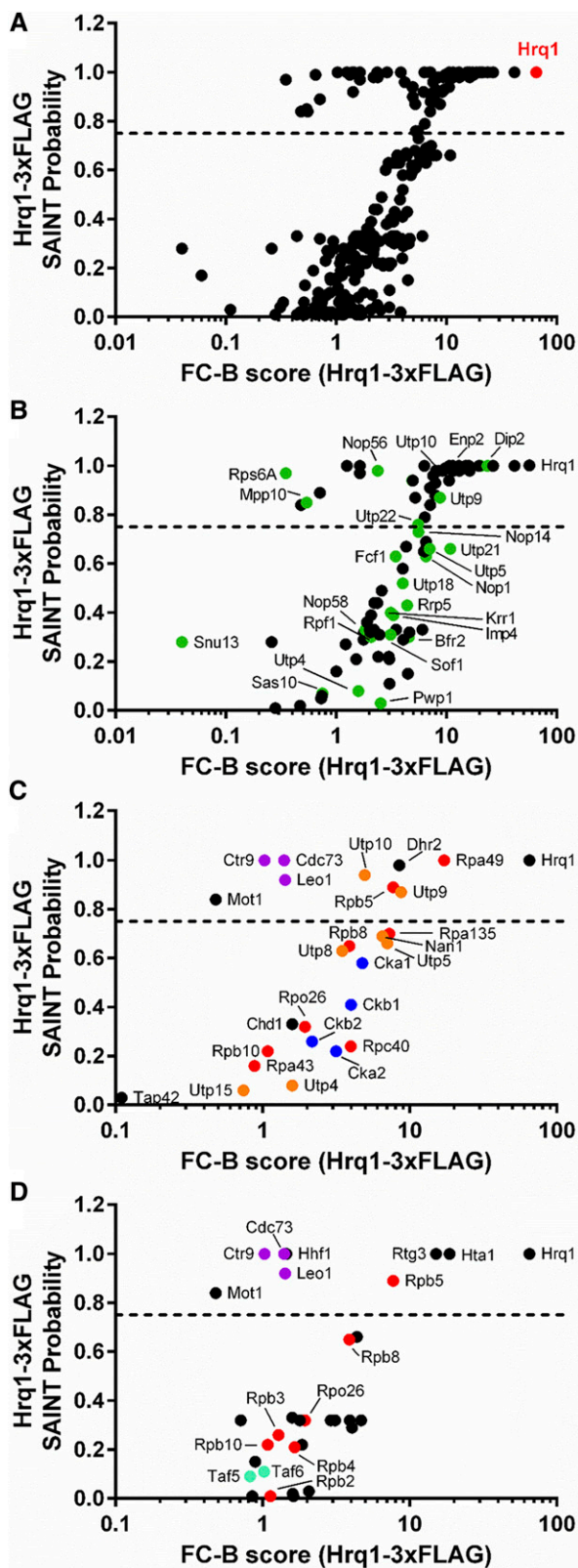


**Figure 1** Identification of the Hrql-3xFLAG interactome by IP-MS and SAINT. A) Overview of the 290 interactions identified by SAINT in anti-FLAG Hrql purifications. The graph compares the FC-B score against the SAINT probability score. The dashed line represents the 0.75 probability cut-off. The highest confidence hit, Hrql, is shown in red. Subsets of the 290 interactors enriched for rRNA processing and ribosomal small subunit biogenesis (B),

genetic effect may be related to the role of Hrql in telomere maintenance (Bochman *et al.* 2014; Nickens *et al.* 2018).

### The physical interactome of Hrql

To complement our genetic analysis of *hrql* alleles, we also sought to identify the proteins that physically interact with Hrql *in vivo*. To do this, we cloned the sequence for a 3xFLAG tag in frame to the 3' end of the *HRQ1* gene, replacing its native stop codon. The tag does not disrupt any known activities of Hrql, as demonstrated by the DNA ICL resistance of the Hrql-3xFLAG strain (Fig. S1 and data not shown). Next, we snap-froze and cryo-lysed cells to preserve macromolecular complexes in near-native states (Mosley *et al.* 2011), immunoprecipitated Hrql-3xFLAG and its associated proteins from the lysates, and analyzed them using a quantitative proteomics approach.

Overall, 290 interacting proteins were identified (Table S6), 77 of which had a SAINT score > 0.75 and were thus considered significant (Figure 1A). These 77 proteins are enriched for GO Term processes such as rRNA processing, ribosomal small subunit biogenesis, ribosomal large subunit biogenesis, cytoplasmic translation, transcription by RNA polymerase I, transcription by RNA polymerase II, RNA modification, DNA repair, chromatin organization, and peptidyl-amino acid modification (Table 4). Further, these categories are representative of the entire set of 290 proteins.

To demonstrate the robustness of these data, we identified Hrql-interacting proteins that are subunits of larger macromolecular complexes involved in several of the GO Term processes listed above. For instance, among the rRNA processing and ribosomal small subunit biogenesis proteins (Figure 1B), several members of the small ribosomal subunit processome (<https://www.yeastgenome.org/complex/CPX-1604>) are significant Hrql interactors. Many more such proteins had SAINT scores < 0.75, suggesting that they may be secondary interactors (*i.e.*, they physically interact with a significant Hrql interactor rather than Hrql directly) and/or more weakly associated subunits of the processome. Similarly, the transcription by RNA polymerase I (Figure 1C) and transcription by RNA polymerase II (Figure 1D) proteins contain members of multiple macromolecular complexes, including the RNA polymerase I (<https://www.yeastgenome.org/complex/CPX-1664>) and RNA polymerase II (<https://www.yeastgenome.org/complex/CPX-2662>) complexes themselves. As with the *hrql* SGA data in our companion manuscript (Sanders, Nguyen, *et al.*; manuscript #401709), these links to transcription are intriguing and reminiscent of the links of human RECQL5 to transcription (Aygun *et al.* 2008; Izumikawa *et al.* 2008; Saponaro *et al.* 2014).

Despite knowing some mechanistic details of how Hrql functions in ICL repair and telomere maintenance (Bochman *et al.* 2014; Rogers *et al.* 2017; Nickens *et al.* 2018; Nickens *et al.* 2019; Rogers *et al.*

transcription by RNA polymerase I (C), and transcription by RNA polymerase II (D) factors are also shown. Members of macromolecular complexes associated with these processes are labeled and color coded: small ribosomal subunit processome (<https://www.yeastgenome.org/complex/CPX-1604>), green; RNA polymerase I (<https://www.yeastgenome.org/complex/CPX-1664>), II (<https://www.yeastgenome.org/complex/CPX-2662>), and III (<https://www.yeastgenome.org/go/GO:0005666>), red; PAF1 complex (<https://www.yeastgenome.org/complex/CPX-1726>), purple; casein kinase 2 (<https://www.yeastgenome.org/complex/CPX-581>), blue; UTP-A complex (<https://www.yeastgenome.org/complex/CPX-1409>), orange; and TFIIID (<https://www.yeastgenome.org/complex/CPX-1642>), teal. All identifiers for these data are included in Table S6.

■ **Table 4 Gene Ontology (GO) Term enrichment of proteins that physically interact with Hrq1**

GO Term (GO ID)	Genes Annotated to the GO Term	GO Term Usage in Gene List	Genome Frequency of Use
rRNA processing (GO:0006364)	BMS1, BUD21, CBF5, CIC1, DBP10, DBP3, DBP9, DHR2, DIP2, ECM16, ENP2, ERB1, ESF1, FUN12, GAR1, KRE33, MAK5, MOT1, MPP10, MRD1, NHP2, NOP56, NOP8, NSA2, NSR1, NUG1, RLP7, ROK1, RPL1A, RPS6A, RPS8A, RRP12, RRP8, TSR1, URB1, UTP10, UTP22, UTP9	38 of 75 genes, 50.67%	352 of 6436 annotated genes, 5.47%
ribosomal small subunit biogenesis (GO:0042274)	BMS1, BUD21, DHR2, DIP2, ECM16, ENP2, FUN12, KRE33, MPP10, MRD1, NSR1, ROK1, RPS19A, RPS6A, RPS8A, RRP12, SGD1, TSR1, UTP10, UTP22, UTP9	21 of 75 genes, 28.00%	149 of 6436 annotated genes, 2.32%
ribosomal large subunit biogenesis (GO:0042273)	CIC1, DBP10, DBP3, DBP9, ERB1, MAK5, NHP2, NOC2, NOP8, NSA2, NUG1, RIX7, RLP7, RPL12A, RPL1A, RRP8, SDA1, URB1	18 of 75 genes, 24.00%	122 of 6436 annotated genes, 1.90%
cytoplasmic translation (GO:0002181)	FUN12, NIP1, RPL12A, RPL1A, RPL23A, RPL43A, RPS19A, RPS25B, RPS6A, RPS8A	10 of 75 genes, 13.33%	201 of 6436 annotated genes, 3.12%
transcription by RNA polymerase I (GO:0006360)	CDC73, CTR9, DHR2, LEO1, MOT1, RPA49, RPB5, UTP10, UTP9	9 of 75 genes, 12.00%	69 of 6436 annotated genes, 1.07%
transcription by RNA polymerase II (GO:0006366)	CDC73, CTR9, HHF1, HTA1, LEO1, MOT1, RPB5, RTG3	8 of 75 genes, 10.67%	536 of 6436 annotated genes, 8.33%
RNA modification (GO:0009451)	AIR2, CBF5, GAR1, KRE33, NHP2, NOP56, PUS1, RRP8	8 of 75 genes, 10.67%	177 of 6436 annotated genes, 2.75%
DNA repair (GO:0006281)	CDC73, CTR9, HTA1, LEO1, PDS5, RFC3	6 of 75 genes, 8.00%	300 of 6436 annotated genes, 4.66%
chromatin organization (GO:0006325)	CTR9, FPR3, FPR4, HHF1, HTA1, LEO1	6 of 75 genes, 8.00%	310 of 6436 annotated genes, 4.82%
peptidyl-amino acid modification (GO:0018193)	CDC73, CTR9, FPR3, FPR4, HHF1, LEO1	6 of 75 genes, 8.00%	244 of 6436 annotated genes, 3.79%

2020a), we still know very little about this protein and what it may be doing *in vivo*. Thus, we took the unbiased approach described above with our proteomic investigation, focusing on wild-type Hrq1 rather than Hrq1-K318A. Although we have been able to use this mutant to learn about ICL repair and telomere maintenance, its utility as an experimental tool to investigate other processes is unknown. However, if we were to perform immunopurification-mass spectrometry (IP-MS) with Hrq1-K318A, we would start with focused experiments, for instance, treating cells with ICL damage to enrich for repair complexes or crosslinking cells, enriching for telomeric repeat DNA, and identifying the associated proteins. Indeed, such experiments are ongoing.

### Transcriptomic perturbations caused by mutation of HRQ1

Due to the links between the Hrq1 and transcription identified through SGA and IP-MS, we decided to determine if the *S. cerevisiae* transcriptome is altered by HRQ1 mutation. First, we tested the effects of the general transcription stressor caffeine (Kuranda *et al.* 2006) on *hrq1Δ* and *hrq1-K318A* cells. As shown in Figure 2A, the *hrq1-K318A* strain was much more sensitive to 10 mM caffeine than wild-type, though the *hrq1Δ* strain displayed little-to-no caffeine sensitivity. To obtain more quantitative data, we performed growth curve experiments for wild-type, *hrq1Δ*, and *hrq1-K318A* cells in the absence and presence of increasing concentrations of caffeine. At high levels of caffeine, the *hrq1Δ* strain was significantly ( $P < 0.0001$ ) more sensitive than wild-type, but again, the *hrq1-K318A* mutant displayed greater sensitivity at a wider range of concentrations (Figure 2B). These data mirror the increased sensitivity of the *hrq1-K318A* strain to DNA ICL damage compared to the *hrq1Δ* mutant (Bochman *et al.*

2014; Rogers *et al.* 2020a), suggesting that the Hrq1-K318A protein is still recruited to its sites of action *in vivo* but somehow disrupts transcription as a catalytically inert roadblock. It should also be noted that Hrq1-K318A protein levels are similar to those of wild-type Hrq1 when expressed from the HRQ1 locus (Bochman *et al.* 2014), so *hrq1-K318A* effects are not due to changes in helicase levels when the protein is mutated.

As a purine analog, caffeine does cause transcriptional stress, but it has pleiotropic effects on yeast cells, affecting multiple biological pathways (Kuranda *et al.* 2006). Thus, more direct assays of the transcriptional response to HRQ1 mutation were needed. To gain a transcriptome-wide perspective, we therefore performed RNA-seq analysis of wild-type, *hrq1Δ*, and *hrq1-K318A* cells. Compared to wild-type, 107 genes were significantly downregulated and 28 genes were significantly upregulated in *hrq1Δ* cells (Table S7). Similarly, 301 and 124 genes were down- and upregulated, respectively, in *hrq1-K318A* cells compared to wild-type. Similar to the SGA and proteomic data sets, the GO Terms of these differentially expressed genes (DEGs) were enriched for processes such as response to chemical, meiotic cell cycle, mitotic cell cycle, rRNA processing, and chromosome segregation (Table S8).

Figure 2C shows the frequency distribution of all of the changes in expression in the *hrq1* cells compared to wild-type, separated by down- and upregulated DEGs for each mutant. Outliers are denoted as single points, representing the transcripts whose abundances changed the most. The expression changes in most DEGs were mild decreases or increases, but several varied greatly from wild-type. As an internal control, we found that the transcription of HRQ1 in *hrq1Δ* cells displayed the largest decrease among all data sets relative to wild-type (Figure 2C).

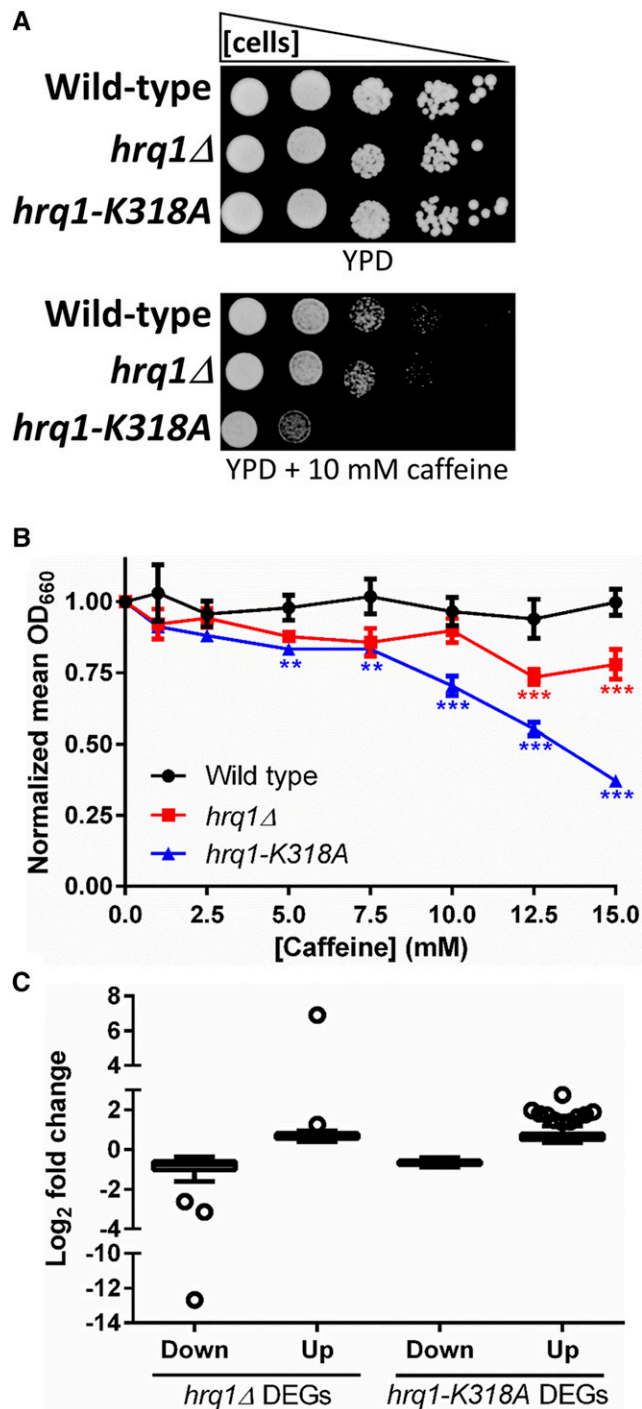


**Figure 2** Mutation of *HRQ1* affects transcription. A) Tenfold serial dilutions of the indicated strains on rich medium (YPD) and YPD containing 10 mM caffeine. The *hrq1-K318A* cells are more sensitive to caffeine than the mild sensitivity displayed by the *hrq1*Δ mutant. B) Quantitative analysis of the effects of caffeine on the growth of *hrq1* cells. The normalized values were averaged from 3 independent experiments and compared to wild-type growth at the same caffeine concentration by one-way ANOVA. \*\*,  $P < 0.001$  and \*\*\*,  $P < 0.0001$ . As in (A), *hrq1*Δ cells display milder sensitivity to caffeine than *hrq1-K318A* cells. C) Analysis of the distribution of the magnitudes of expression changes of the DEGs. The log<sub>2</sub> fold change data for the significantly downregulated (Down) and upregulated (Up) DEGs in *hrq1*Δ and *hrq1-K318A* cells compared to wild-type cells are shown

The largest number of outliers were the 10 upregulated DEGs in *hrq1-K318A* cells. These included genes encoding two cell wall mannoproteins (*TIP1* and *CWP1*) (Van Der Vaart *et al.* 1995; Fujii *et al.* 1999), a heat shock protein (*HSP30*) (Piper *et al.* 1997), a protein required for viability in cells lacking mitochondrial DNA (*ICY1*) (Dunn and Jensen 2003), a predicted transcription factor whose nuclear localization increases upon DNA replication stress (*STP4*) (Tkach *et al.* 2012), a protein of unknown function whose levels increase in response to replication stress (*YER053C-A*), a factor whose over-expression blocks cells in G1 phase (*CIP1*) (Ren *et al.* 2016), and three proteins of unknown function that are induced by ICL damage (*YLR297W*, *TDA6*, and *FMP48*) (Dardalhon *et al.* 2007). No mutations in these 10 DEGs were significant genetic interactors with *hrq1* (Sanders, Nguyen, *et al.*; companion manuscript #401709), but the latter are particularly tantalizing nonetheless considering the known function of Hrq1 in ICL repair (Bochman 2014; Rogers *et al.* 2017; Rogers *et al.* 2020a).

Perhaps the *YLR297W*, *TDA6*, and *FMP48* gene products function in the Hrq1-Pso2 ICL repair pathway, and their levels must be elevated to compensate for the catalytically crippled Hrq1-K318A mutant. Alternatively, they may represent members of a back-up ICL repair pathway that is activated when the Hrq1-Pso2 pathway is ablated. In either case, it should be noted that the RNA-seq experiments were performed in the absence of exogenous ICL damage, but the *hrq1-K318A* cells appear already primed to deal with ICLs in the absence of functional Hrq1. The reasons for this are currently unknown, but our ongoing experiments are addressing this phenomenon. It should also be noted that these three genes were likewise upregulated in the *hrq1*Δ samples (File S4), though not to the same extent as in *hrq1-K318A* cells.

## CONCLUSIONS AND PERSPECTIVES

Here, we used a multi-omics approach to comprehensively determine the *S. cerevisiae* Hrq1 interactome. The data reported here and in our companion manuscript (Sanders, Nguyen, *et al.*; manuscript #401709) greatly expand the known genetic and physical interaction landscape of Hrq1 in yeast, including synthetic genetic interactions with and transcriptomic changes caused by the strong *hrq1-K318A* allele. Various links to the known and putative roles of Hrq1 and its homologs in DNA repair, telomere maintenance, and the mitochondria were found, as well as novel connections to the cytoskeleton and transcription.

Our concurrent data also indicate that the second *S. cerevisiae* RecQ family helicase, *Sgs1*, is likewise involved in transcription (Sanders, Nguyen, *et al.*; manuscript #401709). However, it is unclear if Hrq1 and *Sgs1* act together during transcription or have distinct roles, and it is unknown what these roles are. Human RECQL5 physically interacts with RNA polymerase II, controlling transcription elongation (Saponaro *et al.* 2014). It may also function at the interface of DNA repair and transcription by helping to resolve replication-transcription conflicts (Hamadeh and Lansdorp 2020). It is reasonable to hypothesize that Hrq1 and/or *Sgs1* function

as box and whisker plots drawn using the Tukey method. The individually plotted points outside of the inner fences represent outliers (*i.e.*, expression changes with the largest absolute values) and correspond to genes whose log<sub>2</sub> fold change value is less than the value of the 25<sup>th</sup> quartile minus 1.5 times the inter-quartile distance (IQR) for downregulation or genes whose log<sub>2</sub> fold change value is greater than the value of the 75<sup>th</sup> quartile plus 1.5IQR for upregulation.

similarly and, in the case of Hrq1, perhaps in the transcription-coupled repair of DNA ICL lesions. Future work should address these hypotheses, as well as the others raised throughout this manuscript, to further characterize the roles of RecQ helicases in the maintenance of genome integrity. Similar to the mechanistic identification of the roles of Hrq1 in yeast (Bochman 2014; Nickens *et al.* 2018; Rogers *et al.* 2020a), we anticipate that these data will spur additional research into exciting and unexpected functions of RecQ4 subfamily helicases.

## ACKNOWLEDGMENTS

We thank Amy Caudy for sharing plasmids, the University of Toronto for performing the SGA analyses, Michael Costanzo and members of the Boone lab for help with data collection and interpretation, and members of the Bochman and Mosley labs for critically reading this manuscript. This research was supported by the College of Arts and Sciences, Indiana University (to MLB), the Indiana University Collaborative Research Grant fund of the Office of the Vice President for Research (to MLB and ALM), the American Cancer Society (RSG-16-180-01-DMC to MLB), and the National Institutes of Health (1R35GM133437 to MLB).

*Note added in proof:* See 4359-4368 in this issue for a related work.

## LITERATURE CITED

- Abdelhaleem, M., 2010 Helicases: an overview. *Methods Mol. Biol.* 587: 1–12.
- Andis, N. M., C. W. Sausen, A. Alladin, and M. L. Bochman, 2018 The WYL Domain of the PIF1 Helicase from the Thermophilic Bacterium *Thermotoga elfii* is an Accessory Single-Stranded DNA Binding Module. *Biochemistry* 57: 1108–1118. <https://doi.org/10.1021/acs.biochem.7b01233>
- Aygun, O., J. Svejstrup, and Y. Liu, 2008 A RECQ5-RNA polymerase II association identified by targeted proteomic analysis of human chromatin. *Proc. Natl. Acad. Sci. USA* 105: 8580–8584. <https://doi.org/10.1073/pnas.0804424105>
- Bergman, Z. J., X. Xia, I. A. Amaro, and T. C. Huffaker, 2012 Constitutive dynein activity in *She1* mutants reveals differences in microtubule attachment at the yeast spindle pole body. *Mol. Biol. Cell* 23: 2319–2326. <https://doi.org/10.1091/mbc.e12-03-0223>
- Bochman, M. L., 2014 Roles of DNA helicases in the maintenance of genome integrity. *Mol. Cell. Oncol.* 1: e963429. <https://doi.org/10.4161/23723548.2014.963429>
- Bochman, M. L., K. Paeschke, A. Chan, and V. A. Zakian, 2014 Hrq1, a homolog of the human RecQ4 helicase, acts catalytically and structurally to promote genome integrity. *Cell Rep.* 6: 346–356. <https://doi.org/10.1016/j.celrep.2013.12.037>
- Breitkreutz, A., H. Choi, J. R. Sharom, L. Boucher, V. Neduva *et al.*, 2010 A global protein kinase and phosphatase interaction network in yeast. *Science* 328: 1043–1046. <https://doi.org/10.1126/science.1176495>
- Brosh, Jr., R. M., and S. W. Matson, 2020 History of DNA Helicases. *Genes (Basel)* 11: 255.
- Capp, C., J. Wu, and T. S. Hsieh, 2010 RecQ4: the second replicative helicase? *Crit. Rev. Biochem. Mol. Biol.* 45: 233–242. <https://doi.org/10.3109/10409231003786086>
- Choi, D. H., R. Lee, S. H. Kwon, and S. H. Bae, 2013 Hrq1 functions independently of Sgs1 to preserve genome integrity in *Saccharomyces cerevisiae*. *J. Microbiol.* 51: 105–112. <https://doi.org/10.1007/s12275-013-3048-2>
- Choi, D. H., M. H. Min, M. J. Kim, R. Lee, S. H. Kwon *et al.*, 2014 Hrq1 facilitates nucleotide excision repair of DNA damage induced by 4-nitroquinoline-1-oxide and cisplatin in *Saccharomyces cerevisiae*. *J. Microbiol.* 52: 292–298. <https://doi.org/10.1007/s12275-014-4018-z>
- Choi, H., B. Larsen, Z. Y. Lin, A. Breitkreutz, D. Mellacheruvu *et al.*, 2011 SAINT: probabilistic scoring of affinity purification-mass spectrometry data. *Nat. Methods* 8: 70–73. <https://doi.org/10.1038/nmeth.1541>
- Choi, H., G. Liu, D. Mellacheruvu, M. Tyers, A. C. Gingras *et al.*, 2012 Analyzing protein-protein interactions from affinity purification-mass spectrometry data with SAINT. *Curr Protoc Bioinformatics* Chapter 8: Unit8 15. <https://doi.org/10.1002/0471250953.bi0815s39>
- Croteau, D. L., M. L. Rossi, C. Canugovi, J. Tian, P. Sykora *et al.*, 2012 RECQL4 localizes to mitochondria and preserves mitochondrial DNA integrity. *Aging Cell* 11: 456–466. <https://doi.org/10.1111/j.1474-9726.2012.00803.x>
- Dardalhon, M., W. Lin, A. Nicolas, and D. Aeverbeck, 2007 Specific transcriptional responses induced by 8-methoxypsoralen and UVA in yeast. *FEMS Yeast Res.* 7: 866–878. <https://doi.org/10.1111/j.1567-1364.2007.00270.x>
- Dunn, C. D., and R. E. Jensen, 2003 Suppression of a defect in mitochondrial protein import identifies cytosolic proteins required for viability of yeast cells lacking mitochondrial DNA. *Genetics* 165: 35–45.
- Eki, T., 2010 Genome-Wide Survey and Comparative Study of Helicase Superfamily Members in Sequences Genomes, pp. 168–203 in *Advances in Genetics Research*, edited by Urbano, K. V. Nova Science Publishers, Hauppauge, NY.
- Florens, L., and M. P. Washburn, 2006 Proteomic analysis by multidimensional protein identification technology. *Methods Mol. Biol.* 328: 159–175. <https://doi.org/10.1385/1-59745-026-X:159>
- Friederichs, J. M., S. Ghosh, C. J. Smoyer, S. McCroskey, B. D. Miller *et al.*, 2011 The SUN protein Mps3 is required for spindle pole body insertion into the nuclear membrane and nuclear envelope homeostasis. *PLoS Genet.* 7: e1002365. <https://doi.org/10.1371/journal.pgen.1002365>
- Fujii, T., H. Shimoi, and Y. Iimura, 1999 Structure of the glucan-binding sugar chain of Tip1p, a cell wall protein of *Saccharomyces cerevisiae*. *Biochim. Biophys. Acta* 1427: 133–144. [https://doi.org/10.1016/S0304-4165\(99\)00012-4](https://doi.org/10.1016/S0304-4165(99)00012-4)
- Funakoshi, M., and M. Hochstrasser, 2009 Small epitope-linker modules for PCR-based C-terminal tagging in *Saccharomyces cerevisiae*. *Yeast* 26: 185–192. <https://doi.org/10.1002/yea.1658>
- Gallwitz, D., and R. Seidel, 1980 Molecular cloning of the actin gene from yeast *Saccharomyces cerevisiae*. *Nucleic Acids Res.* 8: 1043–1059. <https://doi.org/10.1093/nar/8.5.1043>
- Ghosh, A. K., M. L. Rossi, D. K. Singh, C. Dunn, M. Ramamoorthy *et al.*, 2011 RECQL4, the protein mutated in Rothmund-Thomson syndrome, functions in telomere maintenance. *J. Biol. Chem.* 287: 196–209. <https://doi.org/10.1074/jbc.M111.295063>
- Giaever, G., and C. Nislow, 2014 The yeast deletion collection: a decade of functional genomics. *Genetics* 197: 451–465. <https://doi.org/10.1534/genetics.114.161620>
- Gustafsson, C. M., L. C. Myers, J. Beve, H. Spahr, M. Lui *et al.*, 1998 Identification of new mediator subunits in the RNA polymerase II holoenzyme from *Saccharomyces cerevisiae*. *J. Biol. Chem.* 273: 30851–30854. <https://doi.org/10.1074/jbc.273.47.30851>
- Hamadeh, Z., and P. Lansdorp, 2020 RECQL5 at the Intersection of Replication and Transcription. *Front. Cell Dev. Biol.* 8: 324. <https://doi.org/10.3389/fcell.2020.00324>
- Hickson, I. D., 2003 RecQ helicases: caretakers of the genome. *Nat. Rev. Cancer* 3: 169–178. <https://doi.org/10.1038/nrc1012>
- Izumikawa, K., M. Yanagida, T. Hayano, H. Tachikawa, W. Komatsu *et al.*, 2008 Association of human DNA helicase RecQ5beta with RNA polymerase II and its possible role in transcription. *Biochem. J.* 413: 505–516. <https://doi.org/10.1042/BJ20071392>
- Jin, W., H. Liu, Y. Zhang, S. K. Otta, S. E. Plon *et al.*, 2008 Sensitivity of RECQL4-deficient fibroblasts from Rothmund-Thomson syndrome patients to genotoxic agents. *Hum. Genet.* 123: 643–653. <https://doi.org/10.1007/s00439-008-0518-4>
- Käll, L., J. D. Canterbury, J. Weston, W. S. Noble, and M. J. MacCoss, 2007 Semi-supervised learning for peptide identification from shotgun proteomics datasets. *Nat. Methods* 4: 923–925. <https://doi.org/10.1038/nmeth1113>
- Kamimura, Y., H. Masumoto, A. Sugino, and H. Araki, 1998 Sld2, which interacts with Dpb11 in *Saccharomyces cerevisiae*, is required for

- chromosomal DNA replication. *Mol. Cell. Biol.* 18: 6102–6109. <https://doi.org/10.1128/MCB.18.10.6102>
- Keller, H., K. Kiosze, J. Sachsenweger, S. Haumann, O. Ohlenschlager *et al.*, 2014 The intrinsically disordered amino-terminal region of human RecQL4: multiple DNA-binding domains confer annealing, strand exchange and G4 DNA binding. *Nucleic Acids Res.* 42: 12614–12627. <https://doi.org/10.1093/nar/gku993>
- Kofoed, M., K. L. Milbury, J. H. Chiang, S. Sinha, S. Ben-Aroya *et al.*, 2015 An Updated Collection of Sequence Barcoded Temperature-Sensitive Alleles of Yeast Essential Genes. *G3 (Bethesda)* 5: 1879–1887 (Bethesda). <https://doi.org/10.1534/g3.115.019174>
- Koh, J. L., Y. T. Chong, H. Friesen, A. Moses, C. Boone *et al.*, 2015 CYCLOPs: A Comprehensive Database Constructed from Automated Analysis of Protein Abundance and Subcellular Localization Patterns in *Saccharomyces cerevisiae*. *G3 (Bethesda)* 5: 1223–1232 (Bethesda). <https://doi.org/10.1534/g3.115.017830>
- Kumari, J., M. Hussain, S. De, S. Chandra, P. Modi *et al.*, 2016 Mitochondrial functions of RECQL4 are required for the prevention of aerobic glycolysis-dependent cell invasion. *J. Cell Sci.* 129: 1312–1318. <https://doi.org/10.1242/jcs.181297>
- Kuranda, K., V. Leberre, S. Sokol, G. Palamarczyk, and J. Francois, 2006 Investigating the caffeine effects in the yeast *Saccharomyces cerevisiae* brings new insights into the connection between TOR, PKC and Ras/cAMP signalling pathways. *Mol. Microbiol.* 61: 1147–1166. <https://doi.org/10.1111/j.1365-2958.2006.05300.x>
- Kwon, Y., A. Vinayagam, X. Sun, N. Dephoure, S. P. Gygi *et al.*, 2013 The Hippo signaling pathway interactome. *Science* 342: 737–740. <https://doi.org/10.1126/science.1243971>
- Langmead, B., and S. L. Salzberg, 2012 Fast gapped-read alignment with Bowtie 2. *Nat. Methods* 9: 357–359. <https://doi.org/10.1038/nmeth.1923>
- Leung, G. P., M. J. Aristizabal, N. J. Krogan, and M. S. Kobar, 2014 Conditional genetic interactions of RTT107, SLX4, and HRQ1 reveal dynamic networks upon DNA damage in *S. cerevisiae*. *G3 (Bethesda)* 4: 1059–1069 (Bethesda). <https://doi.org/10.1534/g3.114.011205>
- Lichten, M., 2014 Tetrad, random spore, and molecular analysis of meiotic segregation and recombination. *Methods Mol. Biol.* 1205: 13–28. [https://doi.org/10.1007/978-1-4939-1363-3\\_2](https://doi.org/10.1007/978-1-4939-1363-3_2)
- Liu, Y., 2010 Rothmund-Thomson syndrome helicase, RECQ4: On the crossroad between DNA replication and repair. *DNA Repair (Amst.)* 9: 325–330. <https://doi.org/10.1016/j.dnarep.2010.01.006>
- Love, M. I., W. Huber, and S. Anders, 2014 Moderated estimation of fold change and dispersion for RNA-seq data with DESeq2. *Genome Biol.* 15: 550. <https://doi.org/10.1186/s13059-014-0550-8>
- Machesky, L. M., and K. L. Gould, 1999 The Arp2/3 complex: a multifunctional actin organizer. *Curr. Opin. Cell Biol.* 11: 117–121. [https://doi.org/10.1016/S0955-0674\(99\)80014-3](https://doi.org/10.1016/S0955-0674(99)80014-3)
- Macris, M. A., L. Krejci, W. Bussen, A. Shimamoto, and P. Sung, 2006 Biochemical characterization of the RECQ4 protein, mutated in Rothmund-Thomson syndrome. *DNA Repair (Amst.)* 5: 172–180. <https://doi.org/10.1016/j.dnarep.2005.09.005>
- Mellacheruvu, D., Z. Wright, A. L. Couzens, J. P. Lambert, N. A. St-Denis *et al.*, 2013 The CRAPome: a contaminant repository for affinity purification-mass spectrometry data. *Nat. Methods* 10: 730–736. <https://doi.org/10.1038/nmeth.2557>
- Meyer, R. E., S. Kim, D. Obeso, P. D. Straight, M. Winey *et al.*, 2013 Mps1 and Ipl1/Aurora B act sequentially to correctly orient chromosomes on the meiotic spindle of budding yeast. *Science* 339: 1071–1074. <https://doi.org/10.1126/science.1232518>
- Monnat, Jr., R. J., 2010 Human RECQ helicases: roles in DNA metabolism, mutagenesis and cancer biology. *Semin. Cancer Biol.* 20: 329–339. <https://doi.org/10.1016/j.semcancer.2010.10.002>
- Mosley, A. L., G. O. Hunter, M. E. Sardi, M. Smolle, J. L. Workman *et al.*, 2013 Quantitative proteomics demonstrates that the RNA polymerase II subunits Rpb4 and Rpb7 dissociate during transcriptional elongation. *Mol. Cell. Proteomics* 12: 1530–1538. <https://doi.org/10.1074/mcp.M112.024034>
- Mosley, A. L., M. E. Sardi, S. G. Pattenden, J. L. Workman, L. Florens *et al.*, 2011 Highly reproducible label free quantitative proteomic analysis of RNA polymerase complexes. *Mol Cell Proteomics* 10: M110 000687. <https://doi.org/10.1074/mcp.M110.000687>
- Nickens, D. G., C. M. Rogers, and M. L. Bochman, 2018 The *Saccharomyces cerevisiae* Hrq1 and Pif1 DNA helicases synergistically modulate telomerase activity in vitro. *J. Biol. Chem.* 293: 14481–14496. <https://doi.org/10.1074/jbc.RA118.004092>
- Nickens, D. G., C. W. Sausen, and M. L. Bochman, 2019 The Biochemical Activities of the *Saccharomyces cerevisiae* Pif1 Helicase Are Regulated by Its N-Terminal Domain. *Genes (Basel)* 10: 411. <https://doi.org/10.3390/genes10060411>
- Ononye, O. E., C. W. Sausen, L. Balakrishnan and M. L. Bochman, 2020 Lysine Acetylation Regulates the Activity of Nuclear Pif1. *J Biol Chem.* <https://doi.org/10.1074/jbc.RA120.015164>
- Piper, P. W., C. Ortiz-Calderon, C. Holyoak, P. Coote, and M. Cole, 1997 Hsp30, the integral plasma membrane heat shock protein of *Saccharomyces cerevisiae*, is a stress-inducible regulator of plasma membrane H(+)-ATPase. *Cell Stress Chaperones* 2: 12–24. [https://doi.org/10.1379/1466-1268\(1997\)002<0012:HTIPMH>2.3.CO;2](https://doi.org/10.1379/1466-1268(1997)002<0012:HTIPMH>2.3.CO;2)
- Ren, P., A. Malik, and F. Zeng, 2016 Identification of YPL014W (Cip1) as a novel negative regulator of cyclin-dependent kinase in *Saccharomyces cerevisiae*. *Genes Cells* 21: 543–552. <https://doi.org/10.1111/gtc.12361>
- Rogers, C. M., and M. L. Bochman, 2017 *Saccharomyces cerevisiae* Hrq1 helicase activity is affected by the sequence but not the length of single-stranded DNA. *Biochem. Biophys. Res. Commun.* 486: 1116–1121. <https://doi.org/10.1016/j.bbrc.2017.04.003>
- Rogers, C. M., C. Y. Lee, S. Parkins, N. J. Buehler, S. Wenzel *et al.*, 2020a The yeast Hrq1 helicase stimulates Pso2 translesion nuclease activity and thereby promotes DNA inter-strand cross-link repair. *J. Biol. Chem.* 295: 8945–8957. <https://doi.org/10.1074/jbc.RA120.013626>
- Rogers, C. M., R. H. Simmons Iii, G. E. Fluhler Thornburg, N. J. Buehler, and M. L. Bochman, 2020b Fanconi anemia-independent DNA inter-strand crosslink repair in eukaryotes. *Prog. Biophys. Mol. Biol.* <https://doi.org/10.1016/j.pbiomolbio.2020.08.005>
- Rogers, C. M., J. C. Wang, H. Noguchi, T. Imasaki, Y. Takagi *et al.*, 2017 Yeast Hrq1 shares structural and functional homology with the disease-linked human RecQ4 helicase. *Nucleic Acids Res.* 45: 5217–5230. <https://doi.org/10.1093/nar/gkx151>
- Saponaro, M., T. Kantidakis, R. Mitter, G. P. Kelly, M. Heron *et al.*, 2014 RECQL5 controls transcript elongation and suppresses genome instability associated with transcription stress. *Cell* 157: 1037–1049. <https://doi.org/10.1016/j.cell.2014.03.048>
- Shen, X., G. Mizuguchi, A. Hamiche, and C. Wu, 2000 A chromatin remodelling complex involved in transcription and DNA processing. *Nature* 406: 541–544. <https://doi.org/10.1038/35020123>
- Sikorski, R. S., and P. Hieter, 1989 A system of shuttle vectors and yeast host strains designed for efficient manipulation of DNA in *Saccharomyces cerevisiae*. *Genetics* 122: 19–27.
- Singh, D. K., V. Popuri, T. Kulikowicz, I. Shevelev, A. K. Ghosh *et al.*, 2012 The human RecQ helicases BLM and RECQL4 cooperate to preserve genome stability. *Nucleic Acids Res.* 40: 6632–6648. <https://doi.org/10.1093/nar/gks349>
- Suhasini, A. N., and R. M. Brosh, Jr., 2013 Disease-causing missense mutations in human DNA helicase disorders. *Mutat. Res.* 752: 138–152. <https://doi.org/10.1016/j.mrr.2012.12.004>
- Tkach, J. M., A. Yimit, A. Y. Lee, M. Riffle, M. Costanzo *et al.*, 2012 Dissecting DNA damage response pathways by analysing protein localization and abundance changes during DNA replication stress. *Nat. Cell Biol.* 14: 966–976. <https://doi.org/10.1038/ncb2549>
- Tong, A. H., M. Evangelista, A. B. Parsons, H. Xu, G. D. Bader *et al.*, 2001 Systematic genetic analysis with ordered arrays of yeast deletion mutants. *Science* 294: 2364–2368. <https://doi.org/10.1126/science.1065810>
- Tong, A. H., G. Lesage, G. D. Bader, H. Ding, H. Xu *et al.*, 2004 Global mapping of the yeast genetic interaction network. *Science* 303: 808–813. <https://doi.org/10.1126/science.1091317>

- Uchiyama, F., M. Seki, and Y. Furuichi, 2015 Helicases and human diseases. *Front. Genet.* 6: 39. <https://doi.org/10.3389/fgene.2015.00039>
- Ungar, L., N. Yosef, Y. Sela, R. Sharan, E. Ruppin *et al.*, 2009 A genome-wide screen for essential yeast genes that affect telomere length maintenance. *Nucleic Acids Res.* 37: 3840–3849. <https://doi.org/10.1093/nar/gkp259>
- van der Vaart, J. M., L. H. Caro, J. W. Chapman, F. M. Klis, and C. T. Verrips, 1995 Identification of three mannoproteins in the cell wall of *Saccharomyces cerevisiae*. *J. Bacteriol.* 177: 3104–3110. <https://doi.org/10.1128/JB.177.11.3104-3110.1995>
- Van Maldergem, L., J. Piard, L. Larizza, and L. L. Wang, 1993 Baller-Gerold Syndrome, *GeneReviews*, Vol. R, edited by Adam, M. P., H. H. Ardinger, R. A. Pagon, S. E. Wallace, L. J. H. Bean *et al.*, University of Washington, Seattle, WA.
- Vargas, F. R., J. C. de Almeida, J. C. Llerena, Junior., and D. F. Reis, 1992 RAPADILINO syndrome. *Am. J. Med. Genet.* 44: 716–719. <https://doi.org/10.1002/ajmg.1320440604>
- Walker, B. C., W. Tempel, H. Zhu, H. Park, and J. C. Cochran, 2019 Chromokinesins NOD and KID Use Distinct ATPase Mechanisms and Microtubule Interactions To Perform a Similar Function. *Biochemistry* 58: 2326–2338. <https://doi.org/10.1021/acs.biochem.9b00011>
- Yokoyama, H., D. Moreno-Andres, S. A. Astrinidis, Y. Hao, M. Weber *et al.*, 2019 Chromosome alignment maintenance requires the MAP RECQL4, mutated in the Rothmund-Thomson syndrome. *Life Sci. Alliance* 2: e201800120. <https://doi.org/10.26508/lsa.201800120>

Communicating editor: G. Brown